Ukrainian Journal of Ecology

Effect of climate change on heat waves in the South Sea of Iran

J. Safieh[1]*, D. Rebwar[2], J. Forough[1]

[1]Water Resource Engineering, University of Birmingham, Edgbaston St., B152TT, UK
[2]Department of Hydrogeology, University of Birmingham, Edgbaston St., B152TT, UK
Corresponding author E-mail: javadinejad.saf@ut.ac.ir
Received: 28.08.2020. Accepted: 20.10.2020

The purpose of this research is to identify the heat waves of the South Sea of Iran and compare the conditions in the present and future. To reach this goal, the average daily temperature of 35 years has been used. Also, in order to predict future heat waves, the maximum temperature data of four models of the CMIP5 model series, according to the RCP 8.5 scenario, has been used for the period 2040-2074. In order to reverse the output of the climatic models, artificial neural networks were used to identify the thermal waves, and the Fumiaki index was used to determine the thermal waves. Using the programming in MATLAB software, the days when their temperature exceeded 2 standard deviations as a thermal wave were identified. The results of the research show that the short-term heat waves are more likely to occur. Heat waves in the base period have a significant but poorly developed trend, so that the frequency has increased in recent years. In the period from 2040 to 2074, the frequency of thermal waves has a significant decreasing trend, but usually with low coefficients. However, for some stations from 2040 to 2074, the frequency of predicted heat waves increased.
Keywords: Climate change; Heat waves; RCP 8.5; Climate models; CMIP5

Introduction

The trend of global warming is one of the most important climate change changes of recent decades, which researchers provided on a regional and planetary scale (Cox, 2018). Climate change and global warming, and its consequences for life and the process of development in human societies, have become the greatest global issue. Climate change has caused many phenomena such as storms, floods, thermal waves and frost, in which climate models predict an increase in extreme temperatures in the future (Lhotka, 2018). The IPCC has provided various scenarios for predicting how the greenhouse gas emissions continue to increase, which, according to different scenarios, will double in the course of the 21st century by carbon dioxide. In this regard, there are various ways to predict the future climate, the most comprehensive of which are general circulation models.

The purpose of these models is to simulate all three-dimensional weather features. Generic circulation models (GCMs) can never be used directly for regional predictions. They require a scalable scale to improve local-level predictions by applying local behaviors. The output of the general circulation models can be divided into two types: dynamic and scalable. Heat waves are the most important atmospheric disasters, and the annual mortality rate from climatic hazards shows that thermal waves cause the highest mortality rates compared to other climatic events (Gao, 2018). Reducing the consequences of heat waves depends on identifying thermal waves, their predictions, discovering ways to reduce their effects on general health and identifying areas that are vulnerable to heat waves. So today, one of the most important concerns about climate hazards is the occurrence of heat waves that affect human societies extensively (Zhao, et al. 2018). The incidence and severity of heat waves in parts of the world have increased in recent years (Coquet, et al. 2018). The French heat wave in the summer of 2003, as well as the heat of the summer of 2010, covered a large part of the northern hemisphere such as Russia, Kazakhstan, Iran, China, Africa and parts of Europe. The occurrence of drought and fire in the forests of western Russia and the unprecedented flood event in widespread parts of Pakistan can be cited as the most significant consequences of a severe heat wave in 2010 (Varghese, et al. 2018). Also, heat waves in southeastern Asia have caused mortality in many people in recent years. Due to the increasing global warming in the last decades, there have been studies in the field of thermal wave in the context of climate change studies in different parts of the world (Sherbakov, et al. 2018).

A research of Moriarty, P reviewed the scale of thermal waves in current climate and its model in global warming. The most intense heat wave that occurred in the world was investigated in three periods of time from 1990-1990, 1991-2001, and 2002-2012. The output of multiple hybrid models has been used by different RCP models of the CMIP5 model. Their research shows that in recent decades global warming regions have increased, and in the future, regions like South Asia, North America, South America, Africa and Indonesia will have a one-year bamboo similar to the summer heat wave 2010 Russia anticipates. In another study, the death toll from the Korean wave was predicted. In this study, using the observational data from 1994-2017, the regression analysis method was used to generate time series data from RCP 4.5 and RCP 8.5 through

2060 to derive mortality from heat waves. Their results indicate that the death rate in RCP 4.5 is about 5 times higher and with RCP 8.5 being 7.2 times higher than the baseline. In another study, deaths due to heat waves in Chicago were studied. The results of this study indicate that if the heat wave of the 2003 European heat wave occurs in Chicago in the coming years, in just a few weeks, the annual death rate from heat will be more than 10 times higher. In Iran, the conditions are very sensitive and fragile, because most regions of Iran, especially the southern regions, are inherently dry, so the expansion of heat waves will intensify the persistence of droughts in most areas and cause serious consequences. There are very few studies in the field of thermal wave in Iran. A research of Takada identified the thermal waves with Fumiaki method. Their research results indicate that the short-term heat wave has occurred more. In the north and northwest, the center of Iran and the southern coasts has been a wave of heat. Also, heat waves have been increasing in the course of the current period and have grown richer in recent years. This study aimed to extract and analyze the changes in thermal waves both in the base and future periods on the Gulf coast using a series of CMIP5 models and RCP 8.5 scenarios.

Materials and Methods

The stations studied in this study are in the range of 26 to 30 latitudes and the longitude is from 48 degrees to 56 degrees. Coastal strips are located in different provinces such as Bushehr, Hormozgan and Khuzestan provinces. Selected synoptic stations include Kish, Bandar Abbas and Bushehr port and Abadan (Figure 1).

Fig. 1. Location of stations in the study area.

The data used for the base period from 1980 to 2017 and for the future data is from 2040 to 2074. In this study, for the upcoming data, four climatological models of CMIP5 with RCP 8.5 have been used, which are presented in Table 1. The choice of RCP 8.5 was due to the study of variations in the heat wave in the most greenhouse gas emissions and their heating.

Table 1. Climate models used.

Climate model	The name of center of modeling
Can Esm^2	Canadian Earth system model
MPI-ESM-MR	Max Planck Institution fur meteorologie
CSIRO-MK-3-6-0	Commonwealth scienctific and industrial reaserch organization
CMCC-CESM	CMCC Carbon Earth system model

In this study, for the purpose of descaling the climatic data, the most common type of artificial and neural network, called the MPLS Multilayer Perceptron, has been used. This type of network has a multi-layer perceptron with an input layer of a hidden layer and an output layer, the input data of which is composed of a parameter. These training data are divided into two sub-training data and test data. According to Table 2, training data for Artificial Neural Network includes 74% of the training data and 28% of the test data.

Table 2. Distribute training data in the neural network used.

Classification	Training data	Test data
Number	7306 (74%)	2192 (28%)
Year	1980-2001	2002-2007

According to the following equation, the square root of the error RMSE was calculated for the network outputs for the two sets of testing and training:

$$RMSE = \sqrt{1/N \sum_{n=1}^{N}(q * target - q * output)2} \qquad (1)$$

In which N is the sum of data, and q * target is the dimensionless values in the target set, and q * output is the non-dimensional values of the neural network. For the detection of waves on the Persian Gulf coast, the maximum daily temperature data from 1980 to 2017 and for future years, the maximum daily temperature data for the years 2040 to 2074, using the Fumiaki index, has been used, which can be used with this indicator, warm temperatures Has been identified. To calculate this index, the average of the long-term temperature is calculated for each day of the year so that the daily deviation of each particular day relative to the long-term average will be the basis for the judgment of the day. Average long-term temperatures of each day are obtained by the following equation:

$$T(l,j) = \sum_{1980}^{2017} T(i, j, n)/N \qquad (2)$$

In this case i is the temperature of day i and year n. In order to calculate the daily average of each of the days in question, the average of 35 days from 35 days in particular was taken. To eliminate the noise in the long run, a 9-day moving average filter was performed three times on this data. As a result, the effect of local snapshots on the temperature fluctuation was eliminated. Then, with the help of the following formula, the temperature deviation was calculated for each day of the survey compared to the long-run average.

$$\Delta T = (l, j, n) = T(l,j,n) - T(l, J) \qquad (3)$$

Here ΔT = (I, j, n) is the deviation of day i and the month I and year n compared to the long-term average of the same day. The intensity of the temperature deviation or ΔT depends on the day-to-day variation of temperature and will vary by season and region. So that the values of the deviation of the temperature of different times in a geographical point and in different places at a given time can be compared with each other. It is necessary to standardize these absolute values of temperature deviation using temperature diffraction. As with day-to-day changes, the ΔT diffraction is obtained in 31 days for each day according to the Zero EQ 4 ratio.

Then the 9-day moving average is performed three times.

$$\sigma(l.J) = \sum_{1980}^{2017} \Sigma[\Delta T(l, j, n) - \Delta T(l, j)]2 /31 \, N$$

$$\sigma(l.J) = \sum_{2040}^{2074} \Sigma[\Delta T(l, j, n) - \Delta T(l, j)]2 /31N \qquad (4)$$

$$\Delta T(l.J) = \sum_{1980}^{2017} \Sigma[\Delta T(l, j, n) - \Delta T(l, j)]2 /31 \, N$$

$$\Delta T(l.J) = \sum_{2040}^{2074} \Sigma[\Delta T(l, j, n) - \Delta T(l, j)]2 /31N$$

Finally, the phoenix profile or normalized temperature deviation is calculated from the following equation:

$$X(l,j,n) = \Delta T(l,j,n) / \sigma(l.J)$$

$$\sigma(l.J) = \sqrt{\sigma2 * (l, J)} \qquad (5)$$

After calculating the Fomiaic Index, the days when the NTD coefficient was above 2 and lasted for at least 2 days, the NTD matrix was isolated and was called heat wave.

Results and Discussion
The results and data related to the data deviation of climate models by the neural network are presented for each of the models used in Table 3.

Table 3. Results of climatic models using artificial neural networks.

Climate models	Number of nodes		RMSE					
	Sigmoid function	Sigmoid function	Station 1	Station 2	Station 3	Station 4	Station 5	Average of RMSE
	5	1	9.63	6.14	4.86	4.73	4.53	5.98
	5	1	9.3	7.09	3.92	4.99	4.3	5.92
	15	1	8.77	5.61	3.65	3.4	3.58	5
	10	1	9.21	5.85	3.93	4.73	3.86	5.52

The most precision was the CSIRO-MK3-6-0 model with a mean square error of 4.99 for all stations (average) and the lowest accuracy with the 5.97 Can ESM2 model. The maximum heat wave extracted for base station data is station 1. The intensity of the heat waves was very high in 2010, so that the heat waves of all stations in this year have had the highest incidence. The thermal wave of the basic data, except for station 2, has a significant increase (at 95% level). But this process, except for the 4th, which has a coefficient of 0.58, was poor for other stations and a coefficient of determination of less than 0.23. In general, the course can be divided into 2 sections (1982-1997 and later, see Fig. 2). So, based on the independent T-test, the average of the occurrence of heat waves for all stations in these two periods was statistically significant, and this number was 9.65 for the first period and 15.9 for the subsequent period.
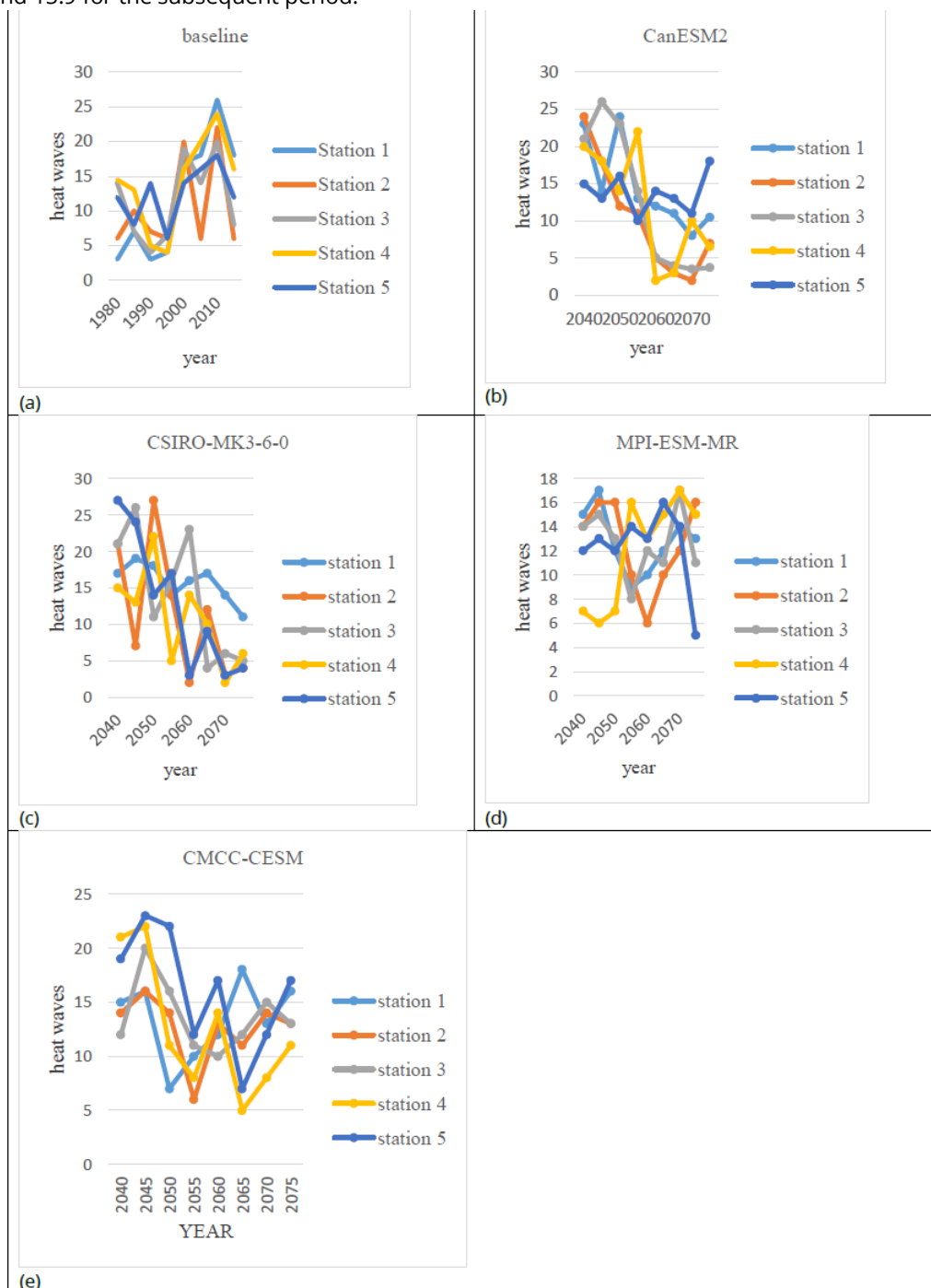

Fig. 2. heat waves from baseline (a) and from climate models of CanESM2 (b), CSIRO-MK3-6-0 (c), MPI-ESM-MR (d), CMCC-CESM (e) for future time.

The frequency of thermal waves from 2 days to 29 days indicates that the short-term heat wave is most frequent. The time series of the thermal waves for the stations examined based on the selected models based on RCP 8.5 and for basic data (fig. 2). According to the CanESM2 model, the highest frequency of heat waves for the future period was extracted for stations 1, 3 and 5, respectively, and the lowest heat wave was extracted for stations 2 and 4, respectively. According to the projections for 2040-2074, with this model, the time series of the frequency of thermal waves for all stations will have significant decreases. This decreasing trend at stations 3 and 5 has the most severe and weakest coefficient of determination, respectively. Despite

the decreasing of the extracted trends, the total number of predicted waves with this model is higher for all stations than the extracted waves for the base data. On a monthly scale, the highest heat waves have been extracted for July. In the meantime, most occurrences form a short-term heat wave from 2 to 11 days, with a 2-day and 5-day heat wave having the highest frequency.

The monthly frequency of thermal waves indicates that the summer season, especially the moon and moon, has the highest thermal wave. In general, the seasonal variation of the thermal wave for baseline data is seasonal and the maximum is detectable for February, April and July to September (Fig. 3).
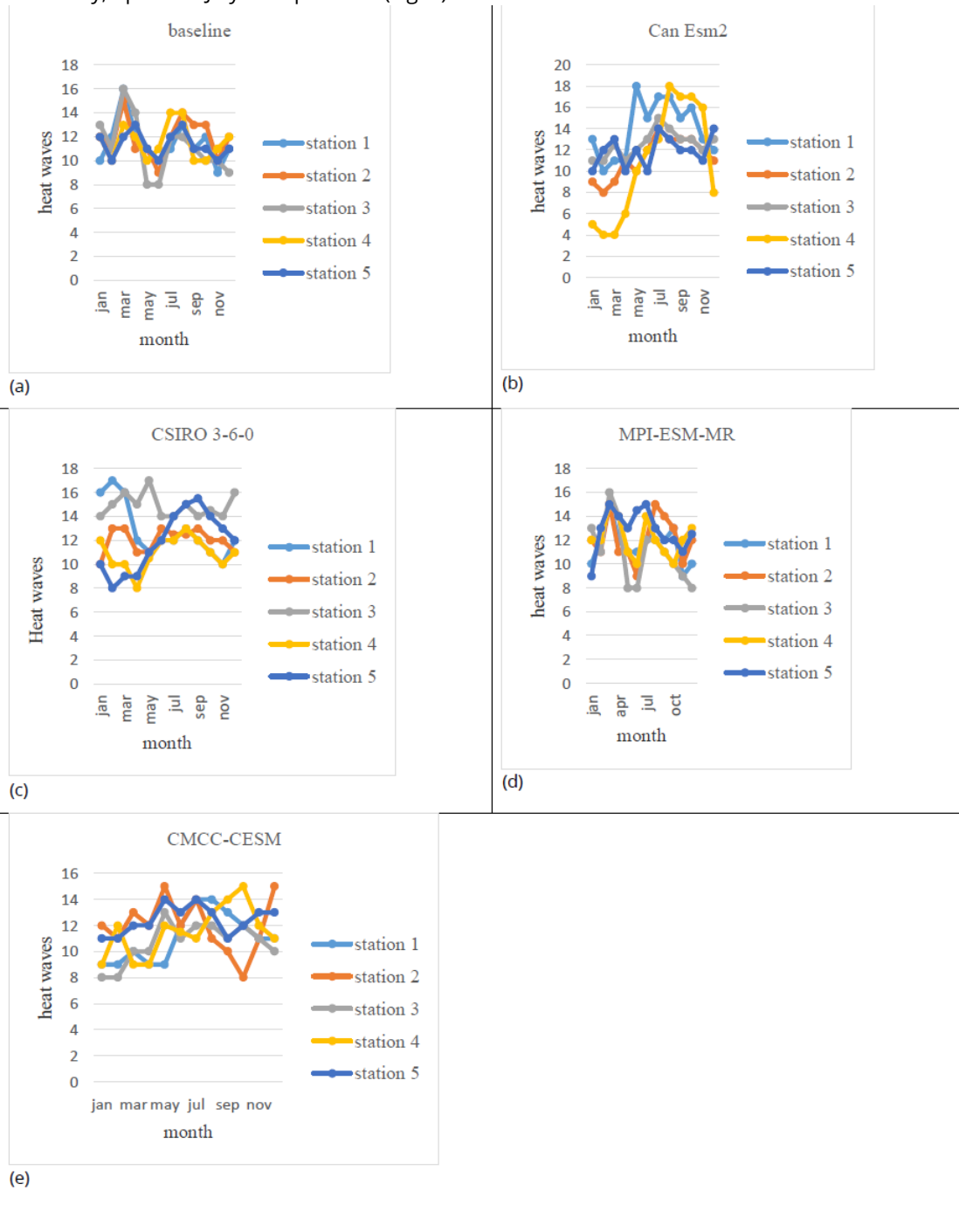

Fig. 3. Monthly changes of heat waves for baseline (a) and for climate models of Can ESM3 (b), CSIRO 3-6-0 (c), MPI-ESM-MR (d), CMCC-CESM (e) for future time period.

According to the MPI-ESM-MR model, the frequency of predicted heat waves is significant for other stations, except for station 4 (non-significant increase trend) for other stations. These trends, except for the Kish station, have a very small coefficient of determination. The highest thermal wave obtained from the MPI-ESM-MR model for the future period is related to station 2 and 5, and the lowest heat wave is related to Station 3. Also, the frequency of predicted heat waves is higher than the base period, and the maximum heat wave extracted in this model is respectively in the months of March, August and July, and the lowest is in November (Figure 3). The most frequent heat wave incidence in this model is the short-wave heat wave, with 2-day waves more frequent at all stations than in other days. For predicted frequencies based on the CSIRO-MK-3-6-0 model, there is a significant decreasing trend in all stations, and the highest coefficient for determining these trends is related to station 5 and the lowest of station 3. Given the frequency of predicted heat waves with this model from 2040 to the middle of the given period, the numbers are large.   In spite of the decreasing processes at all stations, the total number of extracted

waves of stations is higher than the base data. The highest predicted heat waves relate to Stations 3, 2 and 1, and the lowest heat wave associated with station 4. According to this model, in August and then in September, it will have the highest heat wave and the lowest in April (Fig. 3). In fact, the warming waves of the year are the highest. The most frequent heat wave events in this model are short-wave heat waves. The heat wave pattern extracted from the predicted data with the CMCC-CESM model, except for Station 1, has been reduced and significant in other stations. The highest probability of determining these trends for station 1 and the lowest for station 2 is extracted. The CMCC-CESM model is the only model in which the number of predicted waves is lower than the base time data. The highest heat wave extracted by this model is in July and the lowest in February. The most common occurrence of thermal waves in this model is short-wave heat waves, with 2-day waves having the highest share among other waves. Duncan test was used to determine the difference between the frequency of heat waves in the base and future periods, and on the basis of this sample at 0.05, it was found that there is no significant difference between the thermal waves of the base and the future data. The annual variation of the thermal wave in the futures period compared to the base period (Table 4) is that the frequency of heat waves in the future period for the stations of Abadan and Bandar Abbas in canESM2 and CSIRO-MK3-6-0 models 2 stations in MPI-ESM-MR models And CSIRO-MK3-6-0, and the MPI-ESM-MR and CMCC-CESM stations are increasing compared to the base period, but Station 5 in all of the models examined will increase the frequency of thermal waves in the coming years.

Table 4. Comparision heat waves between base line and future data.

Station	Station 1	Station 2	Station 3	Station 4	Station 5
Can Esm2	435	377	442	381	422
MPI-ESM-MR	402	424	406	415	443
CSIRO-MK-3-6-0	449	421	458	389	416
CMCC-CESM	388	407	383	402	443
Baseline	431	408	411	401	400

Seasonal variations in the output of climate models compared to baseline data are presented in Table 5.

Table 5. Seasonally comparison heat waves between base line and future data.

Station	Season	The percentage of heat waves from baseline data	The percentage of heat waves from future data
Station 1	Spring	30.45	24.3
	Summer	30	27.88
	Autumn	17.4	22.62
	winter	22.99	25.49
Station 2	Spring	21.43	24.24
	Summer	26	26.22
	Autumn	28.58	24.83
	winter	25	25.33
Station 3	Spring	21.74	24.71
	Summer	26.82	27.11
	Autumn	25.82	25.18
	winter	24.11	24.64
Station 4	Spring	23.56	23.75
	Summer	23.34	29.83
	Autumn	23.75	25.82
	winter	25.18	20.82
Station 5	Spring	24.28	24.81
	Summer	25.54	28.33
	Autumn	23.36	25.22
	winter	23.11	23.82

At the station, there are many changes in the autumn and winter season, and the amount of heat waves in the coming years will increase in these two seasons from the base period. At the station 2, the heat waves of the spring season have changed a lot and after the spring season, the heat waves in the summer and winter season will be higher than the base period. At station 3 in all seasons except the summer season, the amount of heat waves will be higher than the base period. In station 4, heat waves only show a decrease in winter only, and in the rest of the seasons the heat waves show an increase compared to the base period, and eventually station 5 will increase in all seasons of the year, as compared to the base period.

Conclusion

In this research, following the descent of data from climate models, the thermal waves of the southern shores in two periods of 35 years in the basics and future courses have been identified and identified. Base dangers from 1980 to 2017 have been added to the frequency of thermal waves in the study area and in all stations examined, the incremental process with low-coefficient determination is considered. Also, there is a significant difference between the average number of thermal waves in the first part of the basic data (1984 to 1997) and the second part (1997 to 2017) and the average of the second period of the first period is higher. In other words, in recent years, the occurrence of heat waves has increased. These findings confirm the results of (Raghavendra, et al. 2018). Contrary to the basic data, the process of time series and frequency of future heat waves for all stations and all models is diminishing and meaningful. But, as with basic data, the coefficients for determining these trends are negligible except in a few cases. Altogether, except in the CMCC-CESM model, in other models, the frequency of extracted thermal waves for the next 35 years is more than 35 years old. This increase in the frequency of thermal waves in the future compared to the base period in confirming the results of (Geirinhas, et al. 2019 and Imada, et al. 2019) Fujian Foammatics index is based on temperature deviation from long time mean time of the same time and place, and reinforcement of tropical high pressure due to increasing greenhouse gases and prolonged and severe deployment of it, can be achieved with more heating and More sweeping reduces this deviation from the mean. Of course, more studies are recommended with more models and scenarios.

Aknowledgements

References

Coquet, S., Labadie, M., Vivier-Darrigol, M., Liège, M., & Vandentorren, S. (2018). Early heat wave and heat stroke during distance running, April 2017, France. Revue d'Épidémiologie et de Santé Publique, 66, S341.

Cox, P. M., Huntingford, C., & Williamson, M. S. (2018). Emergent constraint on equilibrium climate sensitivity from global temperature variability. Nature, 553(7688), 319-322.

Gao, M., Yang, J., Wang, B., Zhou, S., Gong, D., & Kim, S. J. (2018). How are heat waves over Yangtze River valley associated with atmospheric quasi-biweekly oscillation. Climate Dynamics, 51(11-12), 4421-4437.

Geirinhas, J. L., Trigo, R. M., Libonati, R., Castro, L. C., Sousa, P. M., Coelho, C. A., ... & Mônica de Avelar, F. M. (2019). Characterizing the atmospheric conditions during the 2010 heatwave in Rio de Janeiro marked by excessive mortality rates. Science of The Total Environment, 650, 796-808.

Imada, Y., Shiogama, H., Takahashi, C., Watanabe, M., Mori, M., Kamae, Y., & Maeda, S. (2018). Climate change increased the likelihood of the 2016 heat extremes in Asia. Bulletin of the American Meteorological Society, 99(1), S97-S101.

Lhotka, O., Kyselý, J., & Farda, A. (2018). Climate change scenarios of heat waves in Central Europe and their uncertainties. Theoretical and applied climatology, 131(3-4), 1043-1054.

Moriarty, P., Honnery, D. (2015). Future cities in a warming world. Futures, 66(1), 45-53.

Raghavendra, A., Dai, A., Milrad, S. M., & Cloutier-Bisbee, S. R. 2019. Floridian heatwaves and extreme precipitation: future climate projections. Climate Dynamics, 52(1-2), 495-508.

Sherbakov, T., Malig, B., Guirguis, K., Gershunov, A., & Basu, R. (2018). Ambient temperature and added heat wave effects on hospitalizations in California from 1999 to 2009. Environmental research, 160, 83-90.

Takada, M., Sotokawa, H., Ishimaru, Y., Imai, T., Ohira, M., Arai, H., ... & Matsuo, Y. (2017). U.S. Patent No. 9,664,452. Washington, DC: U.S. Patent and Trademark Office.

Varghese, B. M., Barnett, A. G., Hansen, A. L., Bi, P., Nairn, J., Rowett, S., ... & Pisaniello, D. L. (2019). Characterising the impact of heatwaves on work-related injuries and illnesses in three Australian cities using a standard heatwave definition-Excess Heat Factor (EHF). Journal of exposure science & environmental epidemiology, 29(6), 821-830.

Zhao, L., Oppenheimer, M., Zhu, Q., Baldwin, J. W., Ebi, K. L., Bou-Zeid, E., ... & Liu, X. (2018). Interactions between urban heat islands and heat waves. Environmental research letters, 13(3), 034003.